

Because of the low counting rates, fairly large spectrometer entrance slits were used. This probably resulted in a variation in the transmission of the spectrometer with electron recoil energy. Such a variation would affect the energy-integrated cross sections  $d\sigma_a/d\Omega$  but not the peak cross sections, since the recoil energies of the electrons in the normalizing proton peaks were the same as those of the maxima of the continua. The error introduced by this effect in the tails of the continua is estimated to be the order of the statistical error in the experimental points defining the tails.

The additional uncertainty in these results due to the other sources of error is estimated to be about five percent in the peak cross sections and 10 or 12% in the energy-integrated cross sections.

#### ACKNOWLEDGMENTS

I would like to express my gratitude to Professor Robert Hofstadter for suggesting this work and for his help and advice. I would like also to express my thanks to the following: S. Sobottka, J. Friedman, and J. Bjorken for several discussions; M. Yearian and G. Ohlsen for help in data-taking; Mrs. S. Ohlsen for setting up the computer program for making radiative corrections to the continua; C. Davey, W. Ewings, E. Wright, and the Hansen Laboratories' machine shop for help in the design and construction of some of the experimental apparatus; M. Ryneveld for help in setting up the experimental equipment; and the operators and crew of the Stanford Mark III Accelerator for providing many hours of successful running time.

### Photodisintegration of the Deuteron from 500 to 900 Mev\*

H. MYERS,† R. GOMEZ, D. GUINIER,‡ AND A. V. TOLLESTRUP  
*California Institute of Technology, Pasadena, California*

(Received July 21, 1960)

The reaction  $\gamma + d \rightarrow p + n$  has been studied for photon energies between 500 and 900 Mev. Bremsstrahlung from the California Institute of Technology electron synchrotron was incident on a liquid deuterium target. Measurements of the energy and angle of the protons arising in the interactions were sufficient to establish that photodisintegration without pion emission occurred and also to determine the energy of the photon which gave rise to the detected proton. An excitation curve was obtained at  $90^\circ$  in the laboratory and angular distributions were measured for photon energies of 500 and 700 Mev. The total cross section decreased smoothly from  $7 \mu\text{b}$  at 500 Mev to  $1 \mu\text{b}$  at 900 Mev.

#### I. INTRODUCTION

THE photodisintegration of the deuteron has been studied extensively from 2.23 Mev to 455 Mev.<sup>1-4</sup> Up to energies of about 10 Mev these experiments provided a complement to low-energy  $n$ - $p$  scattering and radiative capture experiments.<sup>1,2</sup> Between 10 and 200 Mev<sup>2-4</sup> the increasing role played by mesons is observed in a region where such particles exist only in virtual states. Above meson threshold<sup>2-4</sup> photodisintegration experiments are useful as checks on the internal consistency of meson theories.<sup>5</sup> The present experiment

extends the cross-section measurements to 900 Mev. An excitation curve was measured at  $90^\circ$  in the laboratory and angular distributions were obtained for photon energies of 500 and 700 Mev. The results show that the total cross section decreases smoothly from  $7.0 \pm 1.0 \mu\text{b}$  at 508 Mev to  $1.0 \pm 1.0 \mu\text{b}$  at 913 Mev.

#### II. EXPERIMENTAL PROCEDURE

##### General Considerations

The experiment was performed by measuring the energy and angle of protons arising from the reaction

$$\gamma + d \rightarrow p + n. \quad (1)$$

Photons of the bremsstrahlung beam produced by the Caltech electron synchrotron were incident on a liquid deuterium target. Figure 1 is a plan view of the experimental arrangement and Fig. 2 shows details of the telescope.

The angle and energy of the proton determine the kinematics of reaction (1). Since protons arise from reactions other than (1), it is necessary to insure that the observed protons did not come from other processes

\* This work was supported in part by the U. S. Atomic Energy Commission.

† Now at the Cambridge Electron Accelerator, Cambridge, Massachusetts.

‡ Deceased.

<sup>1</sup> J. Blatt and V. F. Weisskopf, *Theoretical Nuclear Physics* (John Wiley & Sons, New York, 1952).

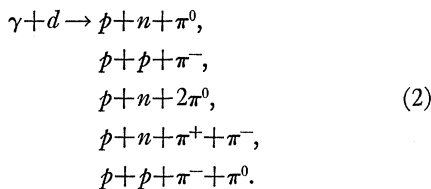
<sup>2</sup> T. Yamagata, M. Q. Barton, A. O. Hanson, and J. H. Smith, *Phys. Rev.* **95**, 574 (1954); E. A. Whalin, *Phys. Rev.* **95**, 1362 (1954); L. Allen, Jr., *Phys. Rev.* **98**, 705 (1955).

<sup>3</sup> J. Keck, R. M. Littauer, G. K. O'Neill, A. M. Perry, and W. M. Woodward, *Phys. Rev.* **93**, 827 (1954).

<sup>4</sup> J. C. Keck and A. V. Tollestrup, *Phys. Rev.* **101**, 360 (1956).

<sup>5</sup> F. Zachariasen, *Phys. Rev.* **101**, 371 (1956).

such as



A method of eliminating protons from the inelastic<sup>6</sup> reactions is obtained by noting that in order to produce a proton with a given vector momentum a higher photon energy is needed in reactions in which pions are produced than in those where the final state consists of only two nucleons. Thus contamination could, in general, be eliminated by setting the peak energy of the bremsstrahlung below the effective threshold for pion production. However, at some energies the energy resolution of the detector was not sufficient to completely separate protons arising in inelastic processes from those arising in the desired elastic process. In such a case the maximum energy of the bremsstrahlung was still set slightly higher than the maximum energy photon which produced elastic protons accepted by the detector. This was done at the expense of counting some inelastic protons. Contributions from inelastic processes were found by measuring the yield per

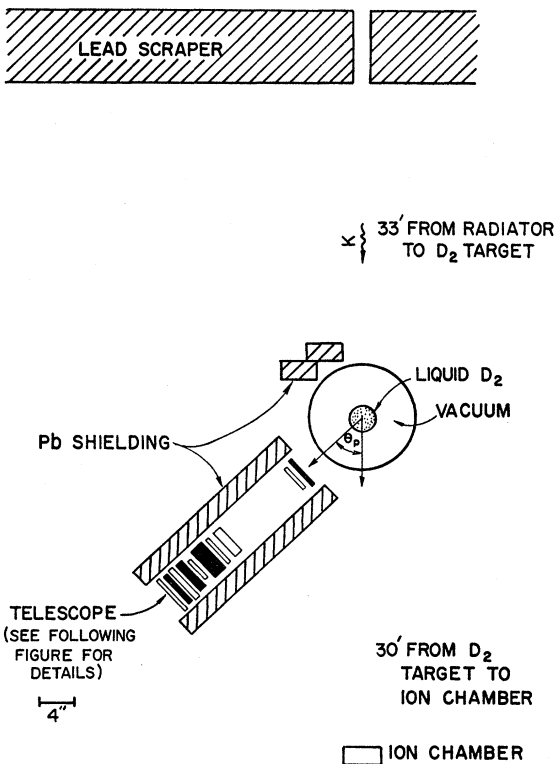


FIG. 1. Plan view of experiment.

<sup>6</sup> In this article we will refer to process (1) as the elastic and to processes (2) as the inelastic photodisintegration.

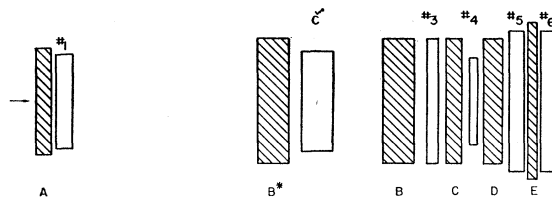


FIG. 2. Plan view of counter telescope. A, B\*, B, C, D, and E are absorbers. 1, 3, 4, 5, and 6 are plastic scintillator counters. C is a Lucite Čerenkov counter.

equivalent quantum as a function of the bremsstrahlung end point. The elastic yield should be independent of the end point as long as the bremsstrahlung spectrum contained all photon energies which could produce elastic protons in the angular and energy range defined by the detector, while the yield from inelastic reactions should increase as the maximum photon energy is raised. This method showed that, within statistics, the inelastic contribution was negligible.

One set of curves in Fig. 3 represents the kinematics for reaction (1). A second set refers to reactions of the type  $\gamma + d \rightarrow p + (n + \pi^0)$  in which neutron and pion are emitted at rest with respect to each other. This corresponds to the case where the minimum photon energy is required to produce a proton with a given vector momentum. The third set is for the reaction  $\gamma + p \rightarrow p + \pi^0$ .

### III. TELESCOPE AND ELECTRONICS

Protons were detected with the six-counter telescope of Fig. 2. Counters 1, 3, 4, 5, and 6 were plastic scintillators and C was a Čerenkov counter made out of UVT Lucite.<sup>7</sup> The telescope was mounted on a movable cart, making it possible to vary the angle which the telescope axis made with the bremsstrahlung beam. Proton energy was determined by an adjustable amount of absorber in the telescope.

Counters 1, 3, 4, and 5 were placed in coincidence, while C and 6 were in anticoincidence. The coincidence-anticoincidence combination of 5 and 6 indicated that particles traversing the telescope had come to rest in either 5 or absorber E. Counters 1, 3, and 4 measured the specific ionization ( $dE/dx$ ) of particles passing through them.

The energy loss in the  $dE/dx$  counters for particles stopping in 5 or E was a function of the mass of these particles. Given the information that a particle had come to rest in 5 or E it was possible to identify that particle as a proton or pion from the energy lost in 1, 3, and 4.

Biases were set on the signals from counters 3 and 4 so that the discriminators corresponding to these counters would be triggered only by pulses which were as large as those expected from protons. A pulse

<sup>7</sup> UVT Lucite has higher transmission in the ultraviolet region and scintillates less than UVA Lucite.

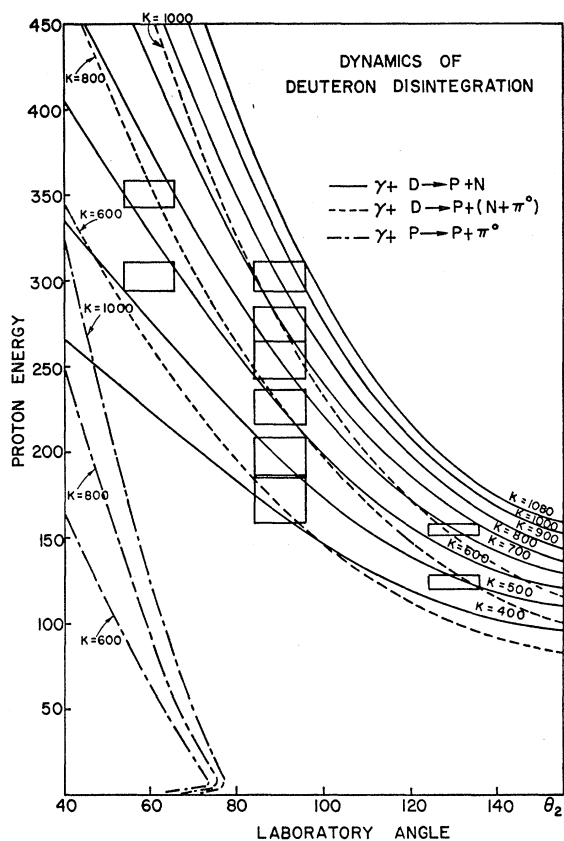


FIG. 3. Proton energy versus proton angle at different photon energies for the reactions:  $\gamma+d \rightarrow p+n$ ;  $\gamma+p \rightarrow p+\pi^0$ ; and  $\gamma+d \rightarrow p+(n+\pi^0)$ . In the latter, pion and neutron are at rest in their center-of-mass system.

occurring in counter 1 was analyzed and recorded in a 20-channel pulse-height analyzer whenever it occurred in coincidence with events in counters 3, 4, and 5 and no event was recorded in counters 6 and  $\bar{C}$ . Figure 4 shows typical pulse-height distributions in counter 1 arising from carbon and deuterium targets. The proton energy corresponded to a range interval between  $R$  and  $R+\Delta R$ . By measuring the proton counting rate from a carbon target as a function of thickness of absorber  $E$ , it was shown that  $\Delta R$  was equal to the thickness of counter 5 plus absorber  $E$  with an error of  $\pm 0.15$  g/cm<sup>2</sup> of copper.<sup>4</sup> This error corresponded to  $\pm 6\%$  of  $\Delta R$  when absorber  $E$  was zero (points 9 and 10 in Table I) and to  $\pm 2\%$  when absorber  $E$  was 5.65 g/cm<sup>2</sup> of copper (points 1 through 8 in Table I).

The Čerenkov counter  $\bar{C}$  was used to reject electrons and pions which might not have been rejected by the pulse-height requirement in counters 1, 3, and 4. The bias on this counter was set sufficiently high so that its discriminator would not be triggered by the small scintillation pulses produced by protons with the appropriate range. The inefficiency introduced by the Čerenkov counter was measured by observing protons from a carbon target and measuring the ratio of the

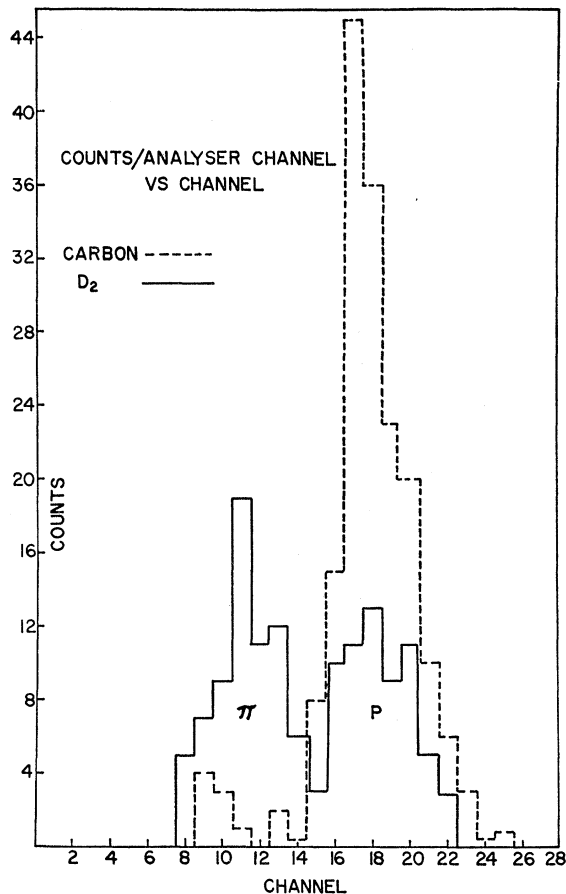


FIG. 4. Typical pulse-height distributions in counter 3 from deuterium and carbon.

number of protons counted with the Čerenkov counter in coincidence to that counted when a pulse from the Čerenkov counter was not required. The bias was set so this ratio would be less than 1%. At this bias setting the efficiency to detect  $\beta=1$  particles was about 95%.

In the telescope pions might have given rise to interactions producing protons which stopped in  $\Delta R$ .

TABLE I. Center-of-mass differential cross sections and corresponding center-of-mass angles for photodisintegration of the deuteron as a function of laboratory angle and laboratory energy. Errors given are due to counting statistics and other uncertainties as discussed in Sec. V.

Point	$k$ (MeV)	$T_p$ (MeV)	$\theta_{lab}$ (deg)	$\theta_{c.m.}$ (deg)	$d\sigma/d\Omega_{c.m.}$ ( $10^{-30}$ cm <sup>2</sup> /sr)
1	438	177	90	109	$1.34 \pm 0.17$
2	513	201	90	111	$0.75 \pm 0.08$
3	614	230	90	113	$0.58 \pm 0.09$
4	716	258	90	114	$0.27 \pm 0.06$
5	793	278	90	116	$0.168 \pm 0.042$
6	913	306	90	118	$0.073 \pm 0.032$
7	503	278	60	80	$0.65 \pm 0.07$
8	646	354	60	82	$0.28 \pm 0.09$
9	510	130	130	145	$0.41 \pm 0.10$
10	734	160	130	148	$0.171 \pm 0.57$

Clearly, by using counters which were placed beyond the point where the proton was produced, it would have been impossible to distinguish between a pion-produced proton and a proton coming from the target. This effect was minimized by placing most of the absorber after counters 1 and  $\bar{C}$ .

The contribution to the proton counting rate due to positive pions, electrons, and photons was measured by running with the target filled with hydrogen at angles and proton energies where difficulties could be expected. It is clear from Fig. 3 that protons produced in hydrogen were kinematically forbidden to enter the telescope with the appropriate energy to be counted. Except at  $\theta=60^\circ$ ,  $T_p=354$  Mev, all runs gave rates which were equal within statistics to the empty-target rates.

At  $T_p=354$  Mev (point 8 in Table I), which was the highest energy proton detected, it was necessary to place sufficient absorber in front of counter  $\bar{C}$  in order to decrease the proton energy at the position of this counter below 320 Mev which is the threshold for production of Čerenkov light in Lucite. Furthermore, counter 1 was not useful at this proton energy to separate protons from pions, because their peaks overlapped almost completely. Thus, before the telescope could differentiate between pions and protons there was an appreciable amount of absorber in which pions could interact and produce protons. The hydrogen run served as the basis for the calculation of the pion contribution to the proton counting rate. This is discussed under Backgrounds in Sec. V.

As another check on the contribution to the proton rate by other particles entering the telescope, runs were taken with the target filled with deuterium at telescope configurations in which protons were kinematically forbidden. The proton counting rate was always the same within statistics to the empty-target rate.

A block diagram of the electronics used is shown in Fig. 5.

IV. DATA COLLECTION

The data were collected during a four-month period. The data for each point were obtained from runs separated by around one week. The equipment was periodically calibrated using a carbon target and setting the telescope at a standard angular position and absorber configuration.

Runs were taken with deuterium, hydrogen, and empty target.

V. DATA REDUCTION

The following corrections and errors were used in obtaining the center-of-mass cross section from the observed counting rates.

Proton Counting Rate

The number of protons detected in each run was obtained from the pulse-height analysis of counter 1.

A typical histogram of the pulse-height distribution is shown in Fig. 4. To obtain the proton counting rate, the counts under the proton peak were counted. An error of  $\pm 5\%$  was ascribed because of the uncertainty due to the overlapping of the proton and pion peaks.

Backgrounds

The empty target rates were subtracted from those obtained in the deuterium runs. The former lay between 10% and 50% of the latter. In addition, at  $\theta=60^\circ$ ,  $T_p=354$  Mev, twice the hydrogen contribution, which amounted to 20% of the foreground, was subtracted from the deuterium rate. This method of subtraction assumed the hydrogen contribution to be due to charged pions. An average  $\pi^-/\pi^+$  ratio of 1.0 at this angle implied that there should be twice as many charged pions per nucleus from deuterium as from hydrogen.

Absorption

The largest correction to the data was for the inelastic interaction of protons in the copper absorber. An absorption measurement made at Berkeley by Richardson *et al.*<sup>8</sup> provided the basis for this correction.

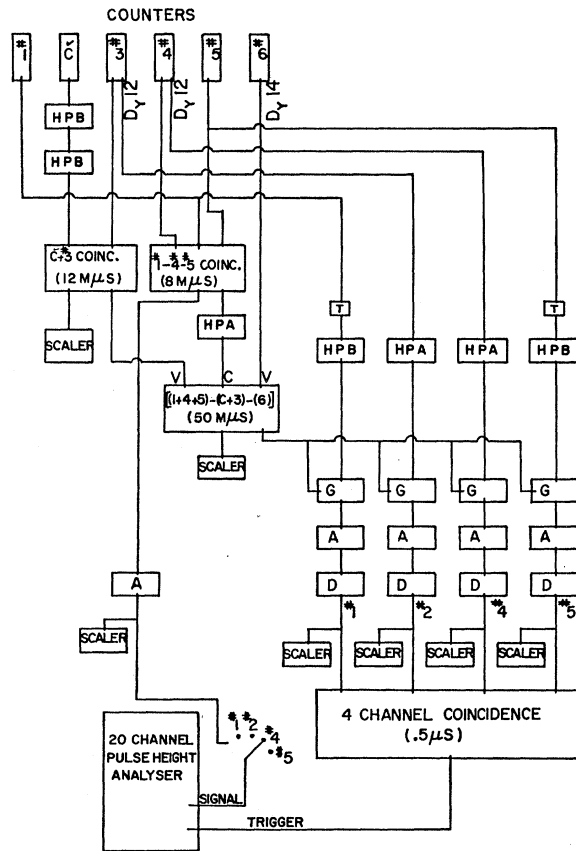


FIG. 5. Electronic block diagram.

<sup>8</sup> R. E. Richardson, W. P. Ball, C. E. Leith, Jr., and B. J. Moyer, Phys. Rev. 86, 29 (1952).

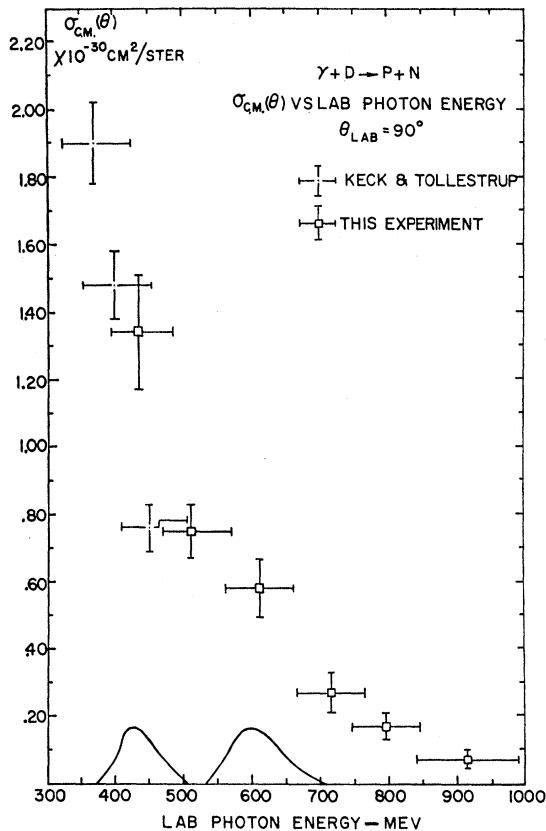


FIG. 6.  $\gamma + d \rightarrow p + n$ . Results of excitation measurement at  $90^\circ$ .

The mean discrepancy between the absorption correction used here and those used by other authors<sup>9</sup> varies between 2% for 127-Mev protons and 10% for 354-Mev protons. An absorption error equal to the mean discrepancy was assigned.

### Scattering

Computations showed that less than 1% of the protons were lost due to large-angle scattering processes except at  $\theta = 60^\circ$ ,  $T_p = 354$  Mev. Here the loss was found to be about 1.5%. An error of 1% is added due to uncertainties in the large-angle scattering calculations. Inefficiencies introduced by multiple Coulomb scattering were calculated and found to be insignificant.

### Solid Angle

An error of  $\pm 2\%$  was introduced to take into account uncertainties in the solid angle.

### Range

$\pm 0.15$  g/cm<sup>2</sup> of copper was assigned as the error in  $\Delta R$ ; this makes an error to the counting rate of  $\pm 2\%$

<sup>9</sup> R. M. Worlock [thesis, Caltech, 1958 (unpublished)] used a correction obtained from a theoretical computation. O. Chamberlain, E. Segrè, R. D. Tripp, C. Wiegand, and T. Ypsilantis [Phys. Rev. **102**, 1695 (1956)] measured an integral absorption curve similar to that of Richardson.<sup>8</sup>

for points 1 through 8 in Table I and of  $\pm 6\%$  for points 9 and 10.

### Deuterium Density

Changes in the amount of hydrogen contamination in the target gave rise to fluctuations in the deuterium density. An error of  $\pm 1\%$  was introduced due to this effect.

### Beam Calibration

The beam was monitored with a 1-inch copper air chamber; this chamber was calibrated using a quantameter built according to the specifications of Wilson.<sup>10</sup> An error of  $\pm 3\%$  was assigned to the beam calibration.

## VI. RESULTS

The reduced data are summarized in Table I. Results of the excitation measurement at  $90^\circ$  in the laboratory are shown in Fig. 6 and the center-of-mass angular distributions for laboratory photon energies of 500 and 700 Mev are shown in Fig. 7. The plotted points of the angular distributions were interpolated or extrapolated from the point at which the measurements had actually

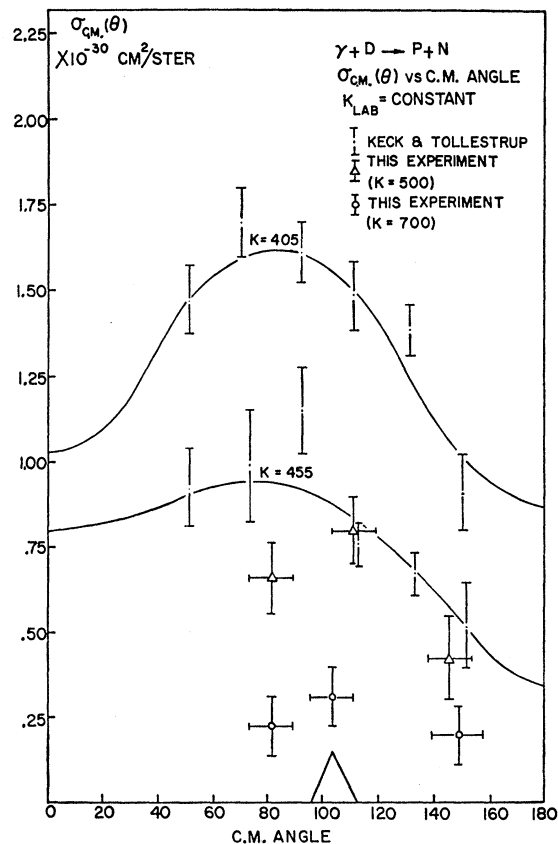


FIG. 7.  $\gamma + d \rightarrow p + n$ . Center-of-mass angular distributions.

<sup>10</sup> R. R. Wilson, Nuclear Instr. **1**, 101 (1957).

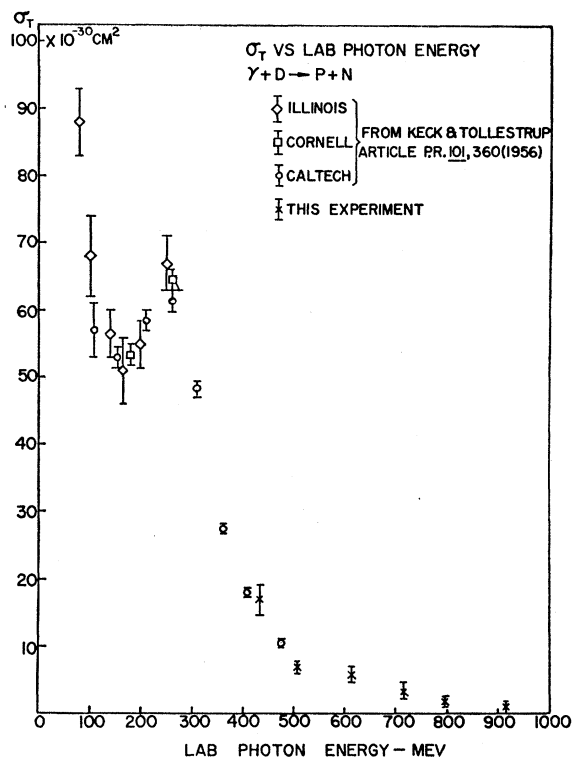


FIG. 8.  $\gamma + d \rightarrow p + n$ . Total cross section from 70 to 900 Mev. See text for discussion.

been made. Assigned energy and angular spreads arising from the finite dimensions of the source and telescope include approximately 80% of the protons which were

counted. Several of the points obtained by Keck and Tollestrup are also shown in Figs. 6 and 7. Figure 8 is the total photodisintegration cross section from 70 to 900 Mev. Total cross sections from the present data were obtained at 500 Mev by integrating a distribution similar to that obtained by Keck and Tollestrup at 455 Mev; at 700, 800, and 900 Mev by assuming isotropy; and at 600 Mev by integrating an angular distribution which is halfway between isotropic and the one used at 500 Mev. These angular distributions are consistent with the data.

Due to the absence of a tractable meson theory, no theoretical work has been done on the deuteron photodisintegration in the energy range of this experiment. A phenomenological calculation like that made by Wilson<sup>11</sup> is not possible because very little is known about the total pion-pair photoproduction cross sections which would make an important contribution in such a calculation. Hence, no comparison with theory has been attempted.

#### ACKNOWLEDGMENTS

The authors wish to thank Professor Robert F. Christy for several valuable discussions concerning the interpretation of the data. The interest of Professor Robert F. Bacher is greatly appreciated. We are very grateful to Mr. Earl Emery for the maintenance of the liquid deuterium target and to Alfred Neubieser, Lawrence Loucks, Daniel Sell, and the crew of the Caltech synchrotron for the efficient operation of the machine.

<sup>11</sup> R. R. Wilson, Phys. Rev. **104**, 218 (1956).